THE JOURNAL OF PHYSICAL CHEMISTRY LETTERS
A JOURNAL OF THE AMERICAN CHEMICAL SOCIETY

pubs.acs.org/JPCL Letter

Quantum Light-Enhanced Two-Photon Imaging of Breast Cancer Cells

Oleg Varnavski, Carolyn Gunthardt, Aasia Rehman, Gary D. Luker, and Theodore Goodson, III*

Cite This: *J. Phys. Chem. Lett.* 2022, 13, 2772−2781 Read Online

ACCESS | Metrics & More | Article Recommendations | Supporting Information

ABSTRACT: Correct biological interpretation from cell imaging can be achieved only if the observed phenomena proceed with negligible perturbation from the imaging system. Herein, we demonstrate microscopic images of breast cancer cells created by the fluorescence selectively excited in the process of entangled two-photon absorption in a scanning microscope at an excitation intensity orders of magnitude lower than that used for classical two-photon microscopy. Quantum enhanced entangled two-photon microscopy has shown cell imaging capabilities at an unprecedented low excitation intensity of ~3.6×10^7 photons/s, which is a million times lower than the excitation level for the classical two-photon fluorescence image obtained in the same microscope. The extremely low light probe intensity demonstrated in entangled two-photon microscopy is of critical importance to minimize photobleaching during repetitive imaging and damage to cells in live-cell applications. This technology opens new avenues in cell investigations with light microscopy, such as enhanced selectivity and time−frequency resolution.

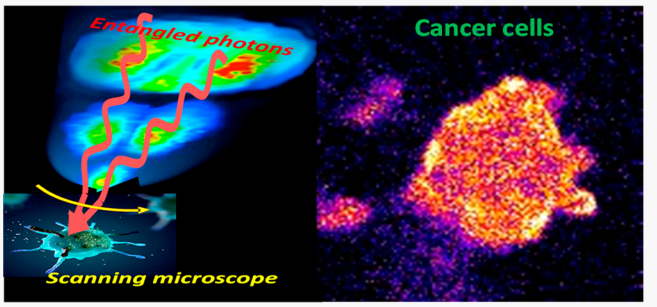

A deeper understanding of complex biological systems requires measuring cellular and molecular-scale events, which are strongly affected by local environmental conditions. Current optical imaging technologies provide direct visualization of biological processes on different time and length scales. However, the high level of light intensity commonly used for such imaging applications (in milliwatt range) can often cause photobleaching and photodamage, substantially disturbing biological processes and functions.[1] These undesirable photochanges can significantly hamper detailed understanding of biological functions, which often require prolonged imaging measurements. Light-induced cell damage is a crucial limitation for light microscopy of living samples, underscoring the critical need to minimize exposure of samples to light. The risk for photodamage to cells requires a delicate imaging balance between maintaining proper functioning of the biosystem and simultaneously extracting useful information. This is especially important for live cell imaging studies in which the duration and frequency of high-intensity light exposure must be adjusted to minimize damaging or altering the function of the system under study.[1,2] While important progress in biological imaging has generally focused on improvements in spatial or temporal resolutions,[3−5] photodamage and photobleaching remain as limiting factors in imaging live cells.[6] Using less probe power for imaging in traditional configuration results in dramatic worsening of signal-to-noise ratio and loss of important biological information. To maintain access to the undisturbed biological information at exposure levels safe for the samples of interest, one needs to go beyond the classical light approach for microscopy and utilize unique properties of nonclassical states of light.

The specific properties of quantum states of light have led to the development of new technologies for observing and controlling matter beyond what is possible classically.[7−13] For example, the nonclassical *NOON* states can beat the shot noise limit in metrology,[13] and while utilizing specific quantum states of light, one can overcome the Rayleigh diffraction limit in imaging.[9,14] Quantum science and technology has the potential to empower microscopy to provide noninvasive and nondestructive imaging of biological systems. Importantly, the key entanglement characteristics of nonclassical light have been shown to remain after propagating through relatively thick, turbid biological samples.[15,16] Using the quantum states of light for illumination, precise phase and linear absorption measurements in a microscopic format have been reported, and precision beyond the standard quantum limit has been achieved in the microscope.[17−19] Significant improvement in signal-to- noise ratio (35%) utilizing quantum enhancement has been recently reported for a coherent Raman microscope

Received: March 8, 2022
Accepted: March 17, 2022
Published: March 23, 2022

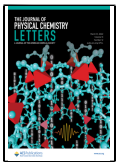

https://doi.org/10.1021/acs.jpclett.2c00695
J. Phys. Chem. Lett. 2022, 13, 2772−2781

utilizing bright quantum correlated illumination.[20] Another approach toward entangled photon microscopy utilizes the enhanced multiphoton absorption of entangled photons. This method was theoretically proposed more than two decades ago[21] but was only recently demonstrated experimentally in organic thin films,[22] suggesting the potential to utilize the entangled two-photon absorption (ETPA) effect for fluorescence microscopy. The ETPA approach focuses on an entirely different class of applications utilizing nonclassical light in comparison with the nonclassical methods providing noise reduction in low-intensity illumination experiments.[17,19] Because of energy−time entanglement, the absorption of entangled photon pairs can be very efficient at low power in comparison with classical, random two-photon absorption, paving the way for low-intensity microscopic two-photon measurements.[10,22−25] The two-photon absorption of entangled photon pairs scales linearly (rather than as a quadratic) in photon flux in this case, just like a one-photon absorption.[10,23−27] This unique property offers a new route toward performing two-photon spectroscopic and microscopic measurements with excitation power much lower than is currently feasible.[8,22−24] Therefore, ETPA can be used as a fundamental mechanism for solving the long-standing challenge of photodamage and phototoxicity in cell imaging.

In this contribution, we report fluorescence microscopy images of breast cancer cells T47D and MCF7 with the probe fluorescence selectively excited in the process of the entangled two-photon absorption in a staining dye. We demonstrated entangled two-photon excited fluorescence images of breast cancer cells collected using the scanning fluorescence microscope at the extremely low probing power of $\sim 3 \times 10^7$ photons/s. We observed microscopic images of 9 different groups of cancer cells in 2 different breast cancer cell lines, immediately after and up to 20 days after fixation, using entangled two photon excitation of fluorescence. Scanning microscopy images of individual breast cancer cells as well as cell clusters were created with nonclassical light excitation at unprecedented low probing intensity. These images were compared with images obtained utilizing classical states of light for one- and two-photon excitation of the dye. The excitation flux used to create the entangled two-photon-excited images of the cells was a factor of $\sim 4 \times 10^6$ lower than that necessary for classical light two-photon excitation to produce the cell image of the same intensity.

In this study, we utilized the MCF7 and T47D epithelial human breast cancer cells to examine biological specimens using quantum light. These adherent tumor cell lines were established in the 1970s from the pleural effusions of two women with estrogen-receptor positive breast cancer.[28,29] These cell lines exhibit a typical cobblestone or polygonal epithelial cell morphology with rounded nuclei and can grow in dense clusters that can form three-dimensional domes when grown on glass or plastic.[28] On average, a single MCF7 cell is approximately 20 μm in diameter but can vary in size depending on the state of the cell cycle and culture conditions. Condensed chromatin, stained with DNA intercalating dyes such as DAPI or Hoechst, appears brighter in mitotic cells compared to cells in the interphase state, in which cells are in an active transcriptional state with overall less compact chromatin. The cell sample preparation protocol is described in Methods and Experimental Details.

ETPA-based microscopy takes the same approach as classical light two-photon excited fluorescence microscopy[3] but uses entangled photon pairs for the excitation.[22] The principal advantage of the microscope based on ETPA is that high intensities are not needed because of strongly enhanced biphoton (entangled photon pair) absorption in comparison with classical (random) two-photon absorption. Energy−time entanglement can result in the ETPA process being more efficient than its classical counterpart.[23,24,30] Importantly, the two-photon absorption of entangled photon pairs scales linearly (rather than as a quadratic) with the photon flux, just like a single-photon absorption.[10,23−27] Qualitatively, both components of an entangled photon pair arrive at the same location almost simultaneously, thereby ensuring enhanced two-photon absorption (and fluorescence) efficiency in the process. This enhancement allows for excitation light intensity much lower than that required for classical light TPA to reach the same fluorescence intensity. ETPA is also a powerful spectroscopic tool that can reveal novel information about complex molecules.[7,8,10,12,30] In order to observe quantum effects in two-photon absorption and fluorescence, it is important to have the photon flux coming out of the spontaneous downconversion unit (SPDC) composed of separated photon pairs or in other words to have less than one photon per spectral mode. This requirement was shown to be met at the excitation entangled photon flux of $\sim 10^7$photons/s in our configuration.[22] Joint spectrum measurements performed on our SPDC have also shown the effective number of occupied Schmidt modes (Schmidt number K) estimated to be greater than 2.5.

Typically for SPDC, there is an interaction Hamiltonian describing the downconversion process that takes into account the nonlinear electric susceptibility tensor of the crystal, $\chi^{(2)}$, and the integral is taken over the volume of the crystal. It involves the electric fields of the involved photon fields, where the electric field of the pump is classical and the fields of the twin beams are quantized:

$$H_{\text{int}}(t) = \varepsilon_0 \int_V \mathrm{d}^3 r \chi^{(2)} E_{\text{p}}^{(+)}(t) E_1^{(-)}(t) E_2^{(-)}(t) + \text{H.c.} \tag{1}$$

With this, the downconverted light can be shown as a twin state, and the superposition of a vacuum state and the twin state is then given as

$$|\psi_{\text{twin}}\rangle = Nl \int\int \mathrm{d}\omega_1 \mathrm{d}\omega_2 \exp\left[-\frac{(\omega_1 + \omega_2 - \omega_{\text{p}})^2}{\Delta\omega_{\text{p}}^2}\right] \text{sinc}\left[\frac{l}{2\pi}(k_1 + k_2 - k_{\text{p}})\right] |\omega_1, \omega_2\rangle \tag{2}$$

where ω_1, k_1 and ω_2, k_2 are the signal and idler frequencies and wavenumbers respectively; l is the length of the nonlinear crystal; and $\Delta\omega_{\text{p}}$ is the spectrum of the pump beam with central frequency ω_{p}. The normalization factor N is given by $N^2 = \frac{T_e\sqrt{2/\pi^3}}{l^2\Delta\omega_{\text{p}}}$.

An accurate calculation of the ETPA process in molecules is a challenging task.[31,32] A recent theoretical study of entangled two-photon absorption in organic chromophores, provides a new insight on the quantitative relation between ETPA and the corresponding classical TPA based on the significantly different line widths associated with entangled and unentangled processes.[32] It predicts substantial enhancement of the two-photon absorption efficiency in comparison with classical light TPA.[32] In a simplified version of the theory, the ETPA process

https://doi.org/10.1021/acs.jpclett.2c00695
J. Phys. Chem. Lett. 2022, 13, 2772−2781

in the staining chromophore can be reasonably approximated using a few dominant excitation pathways[30,31] The ETPA cross section has been theoretically estimated for the absorption of an entangled photon pair generated by a type II down-conversion process.[12,33] For a monochromatic pump source, the entangled two-photon absorption can be expressed as[12]

$$\sigma_e(T_e, \tau) = \frac{\pi\omega_p^2}{\hbar^2\mathcal{E}_0^2c^2A_eT_e}\delta(\varepsilon_f - \varepsilon_i - \omega_p) \left|\sum_i A_i\{2 - \exp[-i\Delta_i(T_e - \tau)] - \exp[-i\Delta_i(T_e + \tau)]\}\right|^2 \quad (3)$$

where A_e and T_e are entanglement area and entanglement time, respectively; ω_p is pump frequency; ε_g and ε_f are the energy of the ground and excited state, respectively; ω_0 is the central frequency of signal and idler photons (degenerate phase-matching conditions); $\Delta_i = \varepsilon_i - \varepsilon_g - \omega_0$ is the detuning energy with i ranging over intermediate energy levels with the energy ε_i; μ_{gi} and μ_{if} are transition dipole matrix elements for gi and if transitions; τ is the variable delay between signal and idler photons; $A_i = D_i/\Delta_i$ with the transition matrix element the dipole moment operator D_i. $D_i = \mu_{gi}\mu_{if}$ where μ_{gi} and μ_{if} are transition dipole matrix elements for gi and if transitions. In eq 3, the terms in σ_e associated with the permanent dipole pathways are neglected.[10,24,31] The entanglement time (T_e), area (A_e), and interphoton delay in the pair τ are critical parameters that are connected to the nonmonotonic absorption process predicted by eq 3 and observed in entangled two-photon experiments.[22−25] It is assumed in eq 3 that the photon pair absorption can take place only within a rectangular time window T_e defined by the nonlinear crystal length and eq 3 holds for $-T_e < \tau < T_e$.[12,33] In our previous entangled two-photon microscopy experiments on organic solid-state films we did observe the nonmonotonic dependence of the image intensity on the time delay between photons of the pair predicted by the eq 3.[22] This delay dependence results from specific quantum interference effects associated with the entanglement.[12,31,33] In this earlier report, we utilized a similar microscopy configuration as the one used in the current work, thus providing a proof of the entangled photon fluorescence origin of the microscopy image.[22]

We performed initial entangled two-photon fluorescence microscopy measurements on drop-cast films of different staining dyes or fluorescent proteins to identify an optimal ETPA label for cells. For these experiments, we prepared drop-cast films of staining dyes DAPI, Hoechst 33342, Hoechst 34580, and green fluorescence protein (GFP). The Hoechst 34580 in a drop-cast film demonstrated the brightest image under our entangled photon fluorescence excitation conditions. The entangled two-photon-produced image of the staining dye Hoechst 34580 in the drop-cast film is shown in Figure S2 (Supporting Information). The Hoechst 34580 image intensity after entangled photon excitation (∼ 7 photons/pixel) in bright spots has demonstrated efficient ETPA followed by a detectable fluorescence. The entangled two-photon fluorescence response in the microscope configuration was found to be comparable with the responses of the other ETPA efficient chromophores under the microscope.[22] Further microscopy experiments on cells stained with the staining dyes DAPI, Hoechst 33342, Hoechst 34580, and GFP showed a clear advantage of using Hoechst 34580 for entangled two-photon imaging.

Hoechst dyes are nonintercalating dyes that bind the DNA minor groove at A-T-rich regions,[43] and their fluorescence increases ∼30 fold upon DNA binding.[44] They have good cell permeability and low cytotoxicity.[44] Fluorescence microscopy of the cells stained with these dyes can provide information about DNA content, its distribution, and the morphology of the cell nucleus that serve as indicators for cell cycle progression. The dye Hoechst 34580 used in our experiments exhibits an emission peak at ∼490 nm and absorption maximum at ∼371 nm.[44] For our initial proof-of-concept experiments with entangled two-photon fluorescence microscopy, we stained living cancer cells with Hoechst 34580 prior to fixation for imaging. Utilizing the scanning microscope with the sample fluorescence excited by the entangled photon beam, we successfully obtained fluorescence images of MCF7 and T47D breast cancer cells. The resolution of 128 × 128 pixels and dwell time of 0.32 ms for each pixel was used to collect a sufficient amount of entangled two-photon excited fluorescence to form the image. For each image, 1000 microscope scan frames were collected and integrated. The total scan time for the cell image was ∼2 h.

The entangled two-photon microscopy images of different cells and groups of MCF7 cells are shown in Figure 1. Nuclei

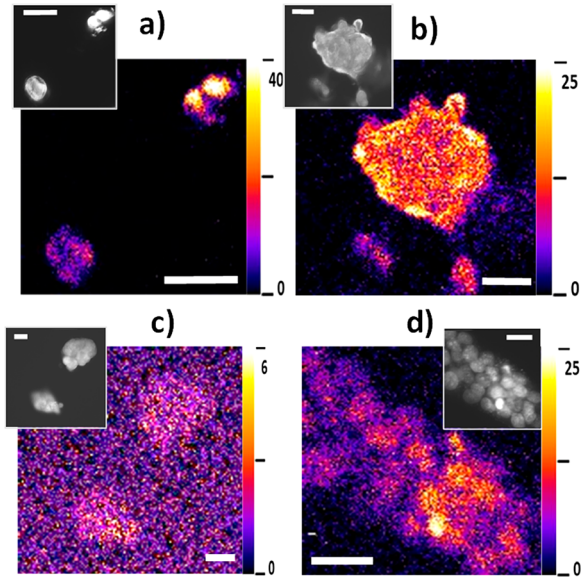

Figure 1. Entangled two-photon light microscopy images of MCF7 cancer cells stained with the dye Hoechst 34580. (a and c) Cells with different numbers of nuclei. (b) Image of a colony of MCF7 cells. (d) Image of large cell cluster. Insets: respective cell images created in fluorescence microscope with the excitation by classical laser light at 405 nm. Spatial scale bar: 20 μm.

of a small cluster of 2−3 cells are visible in the top right corner, and a single cell is in the bottom left of the image in Figure 1a. A large colony of MCF7 cells stained with Hoechst 34580 is imaged with the entangled light fluorescence microscope in Figure 1b. This colony is surrounded by single and pairs of cells clearly resolved in the entangled two-photon induced image. Entangled two-photon fluorescence microscopy was able to resolve internal features of nuclei at an average probing intensity of only 3.6 × 10^7 photons/s. In our experiments, we

https://doi.org/10.1021/acs.jpclett.2c00695
J. Phys. Chem. Lett. 2022, 13, 2772−2781

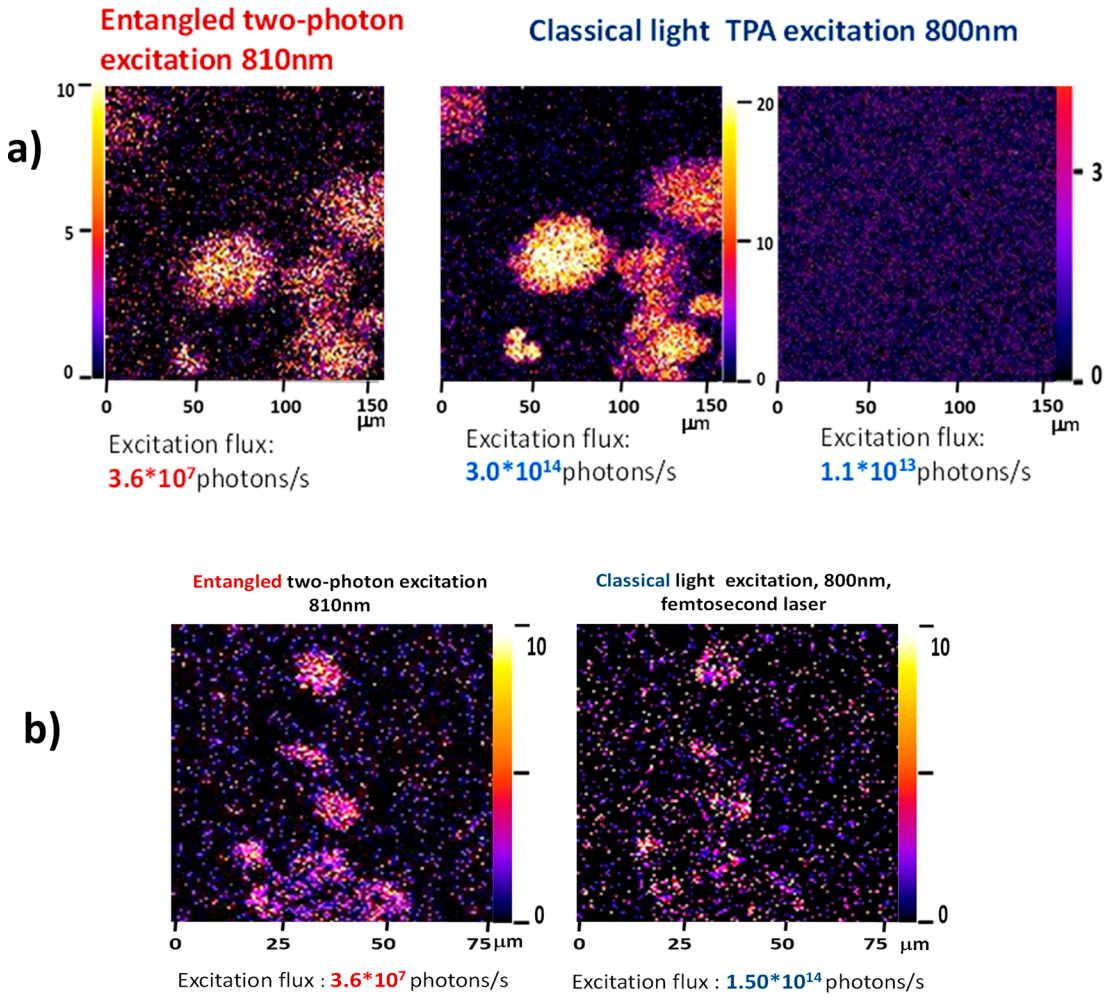

Figure 2. Comparison of cell images (cell line MCF7) created by the entangled photon light with those obtained with classical light for two groups of cancer cells. (a) Microscopy image created by the entangled photons at an intensity of 3.6×10^7 photons/s (left) compared with the images created by the classical TPA process at different excitation intensities. (b) Two-photon fluorescence scanning microscopy images of the same intensity (in photons per pixel) created by classical light (left) and by entangled two photon beam (left). Probe light intensities used in each case are shown under the corresponding images.

have also observed multinucleate cells, which may occur from incomplete cell division in cancer cells.

The entangled two-photon microscopy method also resolved single cells growing in a cluster (Figure 1d). In the entangled two-photon excitation microscope experiments, we collected images in a 128 × 128 square pixel frame with a dwell time of 0.32 ms for each pixel. From 1000 to 4000 image frames were collected in each experiment, and the sum of the signals in each pixel was taken over all collected frames. Under these conditions, the actual background with the empty glass substrate under the microscope was ∼0.6−2.5 photons per pixel, depending on the number of frames and microscope alignment conditions.

We performed a detailed investigation of the relative light excitation intensities used to produce cell images in the microscope to quantify the quantum enhancement factor over the classical TPA microscope. In our setup, it was possible to replace the entangled photon excitation beam with the classical laser beam from the femtosecond laser, ensuring the exact same paths for the two beams (Figure 5). In these experiments, we obtained cell images with entangled light and with classical light using exactly the same microscope and beam configuration in both cases. We also obtained the images under blue light one-photon coherent excitation at 405 nm from the CW laser by removing the interference filter blocking the blue light after SPDC. This allowed us to accurately compare the images created with quantum light with those created by classical photons (Figure 2). We used different sets of neutral filters with precise transmission calibration for attenuation of the classical 800 nm laser beam. In these experiments, we obtained entangled and classical light images of two different groups of cells from different samples (slides) using different microscope settings for magnification and collection time.

Corresponding images for entangled photon and classical light two-photon excitation at different intensities are shown in Figure 2. Imaging with classical two-photon excitation at an average intensity of $\sim 1.1 \times 10^{13}$ photons/s does not produce an image background, while the image created by entangled two-photon excitation at intensity $\sim 3.6 \times 10^7$ photons/s is clearly observed. The classical two-photon image becomes visible only when the intensity increases up to $\geq 5 \times 10^{13}$ photons/s. These results demonstrate a substantial enhancement of two-photon absorption efficiency when going from classical (random) two-photon absorption to the absorption of highly correlated entangled photon pairs. Close inspection of the images obtained at different intensities and microscope

https://doi.org/10.1021/acs.jpclett.2c00695
J. Phys. Chem. Lett. 2022, 13, 2772−2781

settings (pixel dwell time and total collection time) showed that the classical average light flux of ~1.5 × 10^{14} photons/s created an image of the same intensity (in photons/pixel) as that obtained with the entangled photon light having an average photon flux of ~3.6 × 10^{7} photons/s from the new SPDC setup. These photon fluxes correspond to power densities at the sample of 8.6 pW/cm^2 and 4.6 kW/cm^2, respectively. The ratio of classical flux to the entangled photon flux required to produce the same image intensity is close to that obtained with the previous SPDC setup using a femtosecond laser for drop-cast film images of organic material.[22] This result firmly confirms a remarkable enhancement of two-photon absorption efficiency when going from classical (random) two-photon absorption to the absorption of highly correlated entangled photon pairs in the microscope configuration.[22] The corresponding strong reduction of the probing light intensity is a critically important advantage of the ETPA microscope for cell imaging and other biological applications.

Utilizing extremely weak entangled light for the fluorescence excitation, 6 orders of magnitude lower than that used in classical two-photon absorption experiments in the microscope, we were able to image different cell arrangements and stages of mitosis. The entangled two-photon microscope resolved single cells (Figure 1a), multiple nuclei in cells (Figure 1c), and individual cells in large cell colonies and groups (Figure 1b,d). With this new type of nonclassical light microscopy, we were also able to resolve different stages of mitosis for two different lines of cancer cells, T47D and MCF7 (Figure 3). A T47D cancer cell at metaphase has been imaged

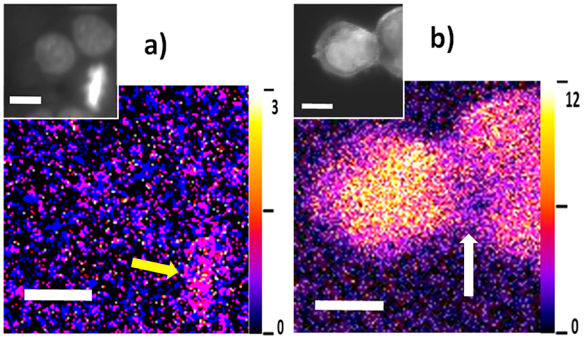

Figure 3. Images of dividing cells obtained with the entangled two-photon microscope at 810 nm. (a) Breast cancer cell line T47D with yellow arrow showing a cell at metaphase. (b) Breast cancer cell line MCF7 with white arrow depicting cells exiting telophase. The reference images obtained with the classical laser light at 405 nm are provided in the insets. Spatial scale bar: 20 μm. Color intensity scales are in photons/pixel.

using the entangled two-photon microscope (Figure 3a). The entangled two-photon-induced image of the chromosomes lined up was relatively weak but clearly recognizable above the background at a probing light intensity of only ~3.6 × 10^{7} photons/s (Figure 3a). Another phase of mitosis—telophase for breast cancer cells MCF7 was imaged using entangled two-photon microscopy (Figure 3b).

We have also checked the photostability of the cell images under entangled two-photon and classical light excitations. With entangled photon fluorescence excitation, no measurable signs of the photochanges (in the image intensity in photons per pixel or in the cell structure) have been detected after ~2 h of entangled light exposure. As mentioned above, the same image intensity was observed for classical excitation light with the average input flux of 1.5 × 10^{14} photons/s (36 μW). The image intensity at this power was relatively low, and each scan took ~2 h (the same as for entangled photon excitation). It was hard to accurately quantify the photodegradation dynamics under these conditions. For classical photodegradation experiments, we used an enhanced average excitation power of a few milliwatts and investigated the degradation dependence as a function of the illumination dose applied to create the fluorescence signal per pixel. In these experiments we observed the classical TPA image intensity dropped down by ~10% after ~10 s of microscopy imaging of 128 × 128 pixels in size and further dropped by factor of 1.5 after ~1 min of the microscope scanning using 3.5 mW classical light for fluorescence excitation. In the classical TPA photodegradation test, we first located the microscope image frame on a particular cell and performed accurate microscope alignment and focusing using fluorescence from the probe in this cell. During the procedure, this cell might be slightly photodegraded. Then we moved the microscope view frame to another cell, which had not been exposed to the fluorescence excitation light before. 50−100 microscope image scans were carried out on this cell, and the image intensity for each scan as a function of the illumination dose was plotted. The result is shown in Figure 4. Clear photobleaching was observed under

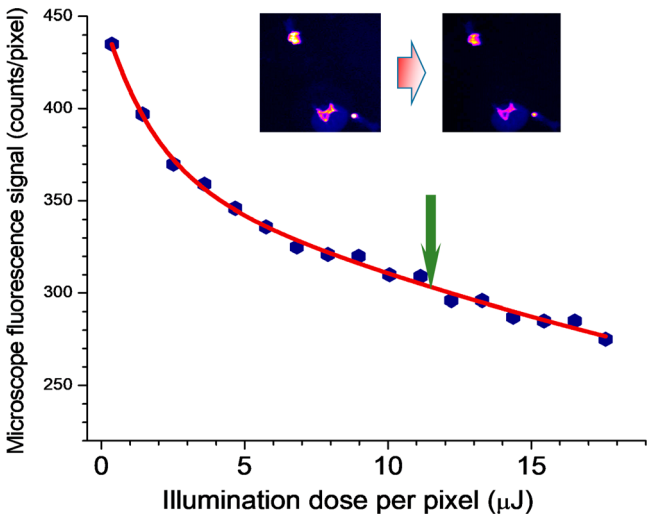

Figure 4. Photodegradation reflected in cell images observed with classical two-photon fluorescence excitation in the scanning microscope as a function of the observation time per pixel. Excitation intensity is 4 mW at the input aperture of the microscope. The arrow indicates illumination dose used in classical TPA experiment having the same image intensity as the ETPA scan (classical image shown in Figure 2b, right). The solid line is a guide for the eye.

two-photon excitation with classical light at 800 nm at the excitation illumination dose of 4.8 × 10^{13} photons/pixel (11.5 μJ per pixel, indicated by an arrow in Figure 4). The same illumination dose was applied to create classical TPA image shown in Figure 2b (left). We note that the illumination dose used in entangled photon imaging (Figure 2b, right) was almost 6 orders of magnitude lower (~2.8 pJ).

We have also performed repetitive reference scans without the excitation light in between actual image collections to make

https://doi.org/10.1021/acs.jpclett.2c00695
J. Phys. Chem. Lett. 2022, 13, 2772−2781

sure that the cell image is stable and reproducible after up to 8 h without exposure to light.

The exposure time for classical light per pixel demonstrated in Figure 4 translates to a total image collection time of ~72 s for image frames of 128 × 128 pixels (see more details in the Supporting Information). With the entangled two-photon imaging of the same cells, we did not see any detectable photochange after 2 h of the image collection time. These results clearly show quantum-enhanced imaging utilizing photodamage-free entangled two-photon scanning microscopy in comparison with the classical light TPA microscopy demonstrating measurable photobleaching in cells. From reports of phototoxicity in the literature, it is known that in the cell subtle phototoxicity may take place long before the cell starts displaying the photobleaching effect or morphological changes.[1,2] It is important to have substantial reduction of the illumination level with respect to that which will induce photobleaching. The quantum-enhanced imaging reported in this contribution provides such capability, reducing the illumination power by orders of magnitude below the level needed for classical TPA microscopy, which shows the photobleaching effect.

In this proof-of-principle work we used the maximum excitation flux of 3.6×10^7 photons/s. This is the highest flux which can be delivered by our pump laser−SPDC system. With this excitation power we were able to collect a microscopy image with a reasonable signal-to-noise ratio in ~2 h, which corresponds to a total illumination dose of ~2.8 pJ/pixel. This collection time is too long for practical measurement in living tissues. However, the excitation flux from the SPDC can be substantially increased using quazi-phase matching in periodically poled nonlinear crystals and more powerful pump lasers. SPDC setups with output fluxes in the range of 10^{10}−10^{14} photons/s have been reported.[34,47−49] An image collection time of ~7 s can be obtained if such high-flux SPDC with the output flux of 10^{10} photons/s is applied to our microscope, as the fluorescence intensity is proportional to the input flux for the entangled two-photon absorption. It is important to note that the illumination dose would remain the same (~2.8 pJ/pixel) because of shorter collection time, implying the same low photodegradation level as for the 10^7 photon/s if the degradation scales linearly with the intensity. The collection time can be further decreased with increased input flux, and the illumination dose will remain the same (~2.8 pJ/pixel). Enhanced input flux can also be used to increase the signal-to-noise ratio of the image, but this can be done at the expense of low illumination dose. The optimal flux can be set as a trade-off between the excitation level that provides good image quality and is safe for the sample.

However, there is a fundamental limitation in the increase of the input entangled photon flux beyond that related to a possible rise of photodegradation in the entangled photon microscope. In order to observe quantum effects in two-photon absorption and fluorescence it is important to have the excitation photon flux composed of separated photon pairs or in other words to have less than one photon per spectral mode. A critical excitation photon flux (Φ_C), defining the crossover between the nonclassical lower-power regime (linear TPA power dependence) and classical light TPA regime (quadratic TPA power dependence), can be estimated from the bandwidth of the downconverted photons Δ_{DC}: $\Phi_C \cong \Delta_{DC}$.[48,37,51] For our SPDC, Δ_{DC} obtained in the joint spectral measurement was found to be ~216 cm^{-1}, which corresponds to $\Phi_C = 6.5 \times 10^{12}$ photons/s. For advanced SPDC based on type I, type 0 phase-matching conditions in properly poled nonlinear crystals or waveguides were reported to provide substantially higher Δ_{DC} and Φ_C.[48−51] This makes it possible to increase the photon flux in the isolated entangled photon pairs (quantum) regime in the microscope well above 10^7 or even 10^{10} photons/s. The above consideration shows that substantial shortening of the image collection time well below 1 s without increase of the illumination dose is feasible for future generations of the ETPA microscope.

This methodology for entangled two-photon microscopy can be used for probing specific signatures in cancer cells. It is well-known that multiple types of heterogeneity exist in primary and metastatic tumors. Heterogeneity is a defining feature of cancer, with primary and metastatic tumors including multiple subpopulations marked by distinct molecular, biochemical, and functional signatures.[45] Identifying and overcoming tumor heterogeneity is paramount to curing cancer. Techniques to detect rare subsets of cancer cells, such as cancer stem-like cells, frequently require dissociation of tissues and large numbers of cells, precluding in situ analysis in intact systems. We envision that nonclassical light can detect subpopulations of cancer cells based on the novel spectroscopic capabilities of quantum light, such as enhanced selectivity for the excitation of a particular state of the molecular probe (either exogenous or endogenous)[11] or the possibility of obtaining ultrafast dynamics information with high spectral resolution.[7,8,10] As this technology advances to live-cell imaging, we also expect the unique properties of nonclassical light will open new capabilities to track the plasticity and evolution of tumor heterogeneity over time. Recent observations of substantial ETPA response from a number of flavoproteins and developments in the theoretical understanding of the enhanced ETPA process suggest new opportunities for performing label-free entangled two-photon microscopy utilizing endogenous probes in cell imaging.[46] The high degree of correlation in entangled states and the resulting quantum interference properties of entangled light may further enable much higher selectivity and new spectroscopic capabilities not achievable by "classical" means.[7,8,10,11,22,24,26,30] For example, high time resolution can be achieved with entangled photons while having narrow spectral selectivity.[7,10] This allows for obtaining new information about intracellular processes hardly accessible with classical light. The quantum nature of light is essential for achieving this degree of time−frequency resolution. In addition, the simultaneous time−frequency resolution may serve as a unique contrast mechanism for a new generation of quantum light imaging. Breast cancer cell imaging with entangled photons excited fluorescence in a scanning microscope has been demonstrated in this contribution. Entangled two-photon microscopy is capable of resolving specific features of breast cancer cells at extremely low probing intensity, including different stages of mitosis. These findings open new promising avenues in biological imaging utilizing a safe, extremely low probing power combined with the novel spectroscopic and selectivity capabilities of the nonclassical states of light.

METHODS AND EXPERIMENTAL DETAILS

In our imaging experiments, we used a custom-built horizontal scanning microscope, which can be excited by nonclassical light produced by a spontaneous downconversion process in a nonlinear BBO crystal. We have coupled the microscope to the

https://doi.org/10.1021/acs.jpclett.2c00695
J. Phys. Chem. Lett. 2022, 13, 2772−2781

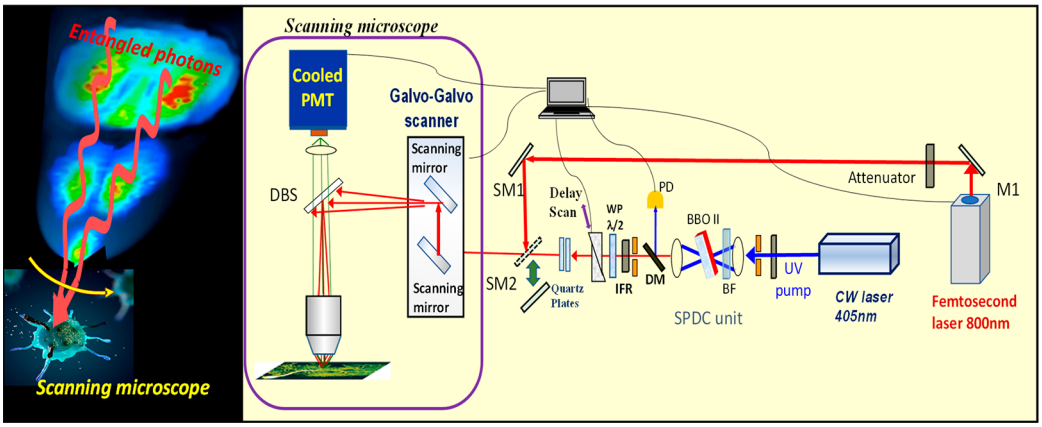

Figure 5. Schematic of the ETPA microscope. Interference filter (IFR) and dichroic mirrors (DMs) separate pump light (405 nm) from entangled photons produced in SPDC. Flipping mirrors SM1 and SM2 direct the classical 800 nm light beam to the microscope for reference experiments with classical light. Pump power references are provided by photodetector (PD). A variable delay between the photons of the downconverted pair is accomplished with the optical delay unit consisting of the $\lambda/2$ wave plate (WP), crystal quarts wedges mounted on the delay stage, and a set of crystal quartz plates. The biphoton beam or classical light undergoes raster scanning in the microscope galvo−galvo scanner. The dichroic beam splitter (DBS) directs the excitation beam to the objective lens. The fluorescent signal from the sample was epi-collected by the microscope objective lens and detected by the cooled PMT.

entangled photon source based on spontaneous down-conversion. Entangled photon pairs were generated in the type II phase matching nonlinear crystal pumped by continuous wave (CW) laser with the center wavelength of 405 nm and the bandwidth of ∼1 nm (see details in this section and the Supporting Information). As compared to the femtosecond pump frequently used in ETPA experiments,[22−24,34] a CW laser has a narrower spectral width, which has been proven to provide a higher degree of frequency entanglement in the SPDC.[30,35,36] The degree of frequency entanglement is an important parameter for efficient ETPA[10,30,37] as well as for the fluorescence microscopy based on ETPA.[22] In our configuration, the SPDC unit was able to produce up to 3.6×10^7 photons/s output flux (singles) when the full power of the DL-405-400 laser was applied for the pump. To characterize the entanglement of the photons produced by SPDC, joint signal-idler frequency spectral (JFS) measurements[38] were performed on a similar type II SPDC with CW pump in a separate setup.[39] These measurements indicated photon frequency anticorrelations with the diagonal spectral width of 20 nm and antidiagonal spectral width <5 nm (upper bound). By performing Schmidt decomposition,[40,41] the effective number of occupied Schmidt modes (Schmidt number K) was estimated to be greater than 2.5 (2.5 is a lower bound, defined by limited spectral resolution of the spectrometer to measure the narrow antidiagonal width of the JFS[39]). A Schmidt number >1 indicates the frequency entanglement in our SPDC (K = 1 if photons are not entangled[41]). The coupling of the SPDC output beam to the microscope has been implemented and optimized to deliver the maximum entangled photon flux to the sample.[22] The BBO crystal was aligned to produce collinear (the two output rings have one intersection) and degenerate spontaneous parametric downconversion.[42] The focal length of the collimating lens directing the entangled photon beam to the entrance aperture of the microscope scanner was adjusted to match the size of the rings' intersection area to the size of the input aperture of the microscope scanner.[22] The light beam from SPDC was directed to the microscope objective lens by a dichroic beam splitter with high reflection at 800 nm and scanned at the overfilled back aperture of a microscope objective lens. Galvo mirrors raster scanned the focus of the objective lens across the sample. The fluorescent signal from the sample was epi-collected by the microscope objective and passed through the dichroic beamsplitter (transparent to visible fluorescence). The fluorescence was detected by a cooled photomultiplier tube (PMT, R7518P, Hamamatsu Photonics) in photon counting regime. The optical system for entangled photon diagnostics at the sample position has been added to the microscope to make sure that we have an excitation beam of good entanglement quality and intensity. The microscope scanner optics were aligned using classical laser light from the CW laser at 405 nm as well as the laser light from femtosecond laser at 800 nm. The classical 800 nm light beam from the femtosecond Mai Tai laser was aligned to match the beam direction of the entangled photon beam from SPDC. This classical beam was used to compare the microscope images created by the entangled photons from SPDC with those obtained via classical two-photon fluorescence excitation mechanism. The classical excitation laser beam in these experiments was heavily attenuated in order to get the TPA fluorescence signals per pixel comparable with those expected for the ETPA excited microscope images.

Cell Samples Used in Experiments and Their Preparation. We obtained MCF7 and T47D human breast cancer cells from the ATCC and cultured cells in DMEM with 10% fetal bovine serum, 1% penicillin/streptomycin, 1% glutamax, and plasmocin (ThermoFisher Scientific, Waltham, MA) at 37 °C in an incubator with 5% CO_2. We plated ∼200,000 cells on glass slides in normal growth medium. After 24 h, we removed slides from growth medium and then fixed adherent cells by submerging slides in 10% neutral-buffered formalin (ThermoFisher Scientific) for 30 min at room temperature. We then washed slides in Hanks' Balanced Salt Solution (HBSS) followed by cell permeabilization in ice-cold methanol for 10 min. Next, we washed slides three times with HBSS and incubated for 15 min at room temperature in the dark with 2 μg/mL of Hoechst 34580 (Sigma-Aldrich, St. Louis, MO). We washed slides three times with HBSS and sealed slides with a coverslip for fluorescence microscopy.

https://doi.org/10.1021/acs.jpclett.2c00695
J. Phys. Chem. Lett. 2022, 13, 2772−2781

.

Scanning Fluorescence Microscope. A custom-built scanning microscope used in this work was based on galvo−galvo scanning head (LSK-GG, Thorlabs Inc.) followed by scanning lenses (Figure 5). The excitation light beam has been directed to the microscope objective lens by a dichroic beam splitter with high reflection at 800 nm and scanned at the overfilled back aperture of a 0.5 NA microscope objective lens (Figure 5). Galvo mirrors raster scanned the focus of the objective lens across the sample. The fluorescent signal from the sample was epi-collected by the microscope objective and passed through the dichroic beamsplitter (transparent to the visible fluorescence). After passing through three filters (FF02−409/LP, FF01−745/SP-25, Semrock Inc., and FEL0450, Thorlabs) cutting scattered light at 400 and 800 nm, the fluorescence is detected by a cooled photomultiplier tube (PMT, R7518P, Hamamatsu Photonics).

Entangled Photon Source. A two-photon quantum state of light at the wavelength 810 nm was generated in the collinear configuration type-II SPDC in a 1 mm thick BBO crystal pumped by continuous wave (CW) laser with the center wavelength 405 nm and the bandwidth ∼1 nm (DL-405−400, CrystaLaser). The nonclassical light produced in the spontaneous downconversion unit (SPDC) was then used for excitation of fluorescence in the scanning microscope. A dichroic mirror (DM) and the interference long pass filter (IF) with the cut on-wave wavelength at 750 nm (FEL0750, Thorlabs Inc.) are used to remove the remaining 405 nm light. Insertion of the second filter FEL0750 did not affect the count rates indicating no leakage of the residual blue light. In our configuration, the SPDC unit was able to produce up to 3.6×10^7 photons/s output flux (singles) when the full power of the DL-405−400 laser was applied for the pump. The coupling of the SPDC output beam to the microscope has been implemented and optimized to deliver the maximum entangled photon flux to the sample.[22] The focusing lens for the SPDC pump had a focal length of 10 cm and has been chosen to obtain the highest output flux from the SPDC. The beam transverse profiles characteristic for the type II SPDC configuration have been observed with the CCD camera installed at the SPDC output port. We tested the corresponding cone intersection structure and adjusted the BBO angle for the best cones intersecting in the collinear geometry.[42,45] The BBO crystal was aligned to produce collinear output (the two output rings have one intersection) and degenerate spontaneous parametric downconversion (Figure S1, Supporting Information). The focal length of the collimating lens directing the entangled photon beam to the entrance aperture of the microscope scanner has been adjusted to match the size of the ring's intersection area and the size of the input aperture of the microscope scanner.[22] The microscope scanner optics were aligned using classical laser light from the CW laser at 405 nm and laser light from femtosecond laser at 800 nm. The classical 800 nm light beam from the femtosecond Mai Tai laser (80 MHz repetition rate, 125 fs pulse length) was aligned to match the beam direction of the entangled photon beam from SPDC. This classical beam was used to compare the microscopy images created by the entangled photons from the SPDC with those obtained via a classical two-photon fluorescence excitation mechanism.

■ ASSOCIATED CONTENT

Supporting Information

The Supporting Information is available free of charge at https://pubs.acs.org/doi/10.1021/acs.jpclett.2c00695.

Scanning fluorescence microscope with entangled photon pair excitation; additional technical details; scan parameters; reference classical light images; more details on cell image photochange under classical and entangled two-photon excitation (PDF)

■ AUTHOR INFORMATION

Corresponding Author

Theodore Goodson, III − *Department of Chemistry and Department of Applied Physics, University of Michigan, Ann Arbor, Michigan 48109, United States;* orcid.org/0000-0003-2453-2290; Phone: 734-647-0274; Email: tgoodson@umich.edu; Fax: 734-615-3790

Authors

Oleg Varnavski − *Department of Chemistry, University of Michigan, Ann Arbor, Michigan 48109, United States*

Carolyn Gunthardt − *Department of Chemistry, University of Michigan, Ann Arbor, Michigan 48109, United States*

Aasia Rehman − *Department of Radiology, University of Michigan, Ann Arbor, Michigan 48109, United States*

Gary D. Luker − *Department of Radiology, Department of Biomedical Engineering, and Department of Microbiology and Immunology, Medical School, University of Michigan, Ann Arbor, Michigan 48109, United States*

Complete contact information is available at: https://pubs.acs.org/10.1021/acs.jpclett.2c00695

Author Contributions

O.V. and C.G. performed most of the experimental work with the microscope; A.R. and G.D.L performed cell preparation and characterization; O.V., G.D.L., and T.G. wrote the manuscript.

Notes

The authors declare no competing financial interest.

■ ACKNOWLEDGMENTS

T.G.III acknowledges support from the U.S. Air Force Office of Scientific Research in the Biophysics Program via Grant FA9550-20-1-0380 and from National Science Foundation through Grant CHE 2004076. G.D.L. acknowledges support from U.S. NIH grants R01CA238042, R01CA238042, U01CA210152, R01CA238023, R33CA225549, and R37CA222563. The authors are grateful to Dr. R. Burdick for sharing the results of SPDC spectral characterization and for valuable discussions.

■ REFERENCES

(1) Laissue, P. P.; Alghamdi, R. A.; Tomancak, P.; Reynaud, E. G.; Shroff, H. Assessing Phototoxicity in Live Fluorescence Imaging. *Nat. Methods.* **2017**, *14*, 657−661.

(2) Icha, J.; Weber, M.; Waters, J. C.; Norden, C. J. Phototoxicity in Live Fluorescence Microscopy, and how to Avoid it. *BioEssays.* **2017**, *39*, 1700003.

(3) Denk, W.; Strickler, J. H.; Webb, W. W. Two-Photon Laser Scanning Fluorescence Microscopy. *Science.* **1990**, *248*, 73−76.

(4) Fornasiero, E. F.; Opazo, F. E. Super-Resolution Imaging for Cell Biologists. *BioEssays.* **2015**, *37*, 436−451.

(5) Winter, P. W.; Shroff, H. P. Faster Fluorescence Microscopy: Advances in High Speed Biological Imaging. *Curr. Opin. Chem. Bio.* **2014**, *20*, 46−53.
(6) Waldchen, S.; Lehmann, J.; Klein, T.; van de Linde, S.; Sauer, M. Light-Induced Cell Damage in Live-Cell Superresolution Microscopy. *Sci. Rep.* **2015**, *5*, 15348.
(7) Dorfman, K. E.; Schlawin, F.; Mukamel, S. Nonlinear Optical Signals and Spectroscopy with Quantum Light. *Rev. Mod. Phys.* **2016**, *88*, No. 045008.
(8) Mukamel, S.; et al. Roadmap on Quantum Light Spectroscopy. *J. Phys. B-At. Mol. Opt.* **2020**, *53*, No. 072002.
(9) Boto, A. N.; Kok, P.; Abrams, D. S.; Braunstein, S. L.; Williams, C. P.; Dowling, J. P. Quantum Interferometric Optical Lithography: Exploiting Entanglement to Beat the Diffraction Limit. *Phys. Rev. Lett.* **2000**, *85*, 2733−2736.
(10) Schlawin, F.; Dorfman, K. E.; Mukamel, S. Entangled Two-Photon Absorption Spectroscopy. *Acc. Chem. Res.* **2018**, *51*, 2207−2214.
(11) Oka, H. Enhanced Vibrational-Mode-Selective Two-Step Excitation Using Ultrabroadband Frequency-Entangled Photons. *Phys. Rev. A* **2018**, *97*, No. 063859.
(12) Saleh, B. E. A.; Jost, B. M.; Fei, H. B.; Teich, M. C. Entangled-Photon Virtual-State Spectroscopy. *Phys. Rev. Lett.* **1998**, *80*, 3483−3486.
(13) Dowling, J. H. Quantum Optical Metrology − the Lowdown on High − NOON States. *Contemp. Phys.* **2008**, *49*, 125−143.
(14) Tenne, R.; Rossman, U.; Rephael, B.; Israel, Y.; Krupinski-Ptaszek, A.; Lapkiewicz, R.; Silberberg, Y.; Oron, D. R. Super-Resolution Enhancement by Quantum Image Scanning Microscopy. *Nat. Photonics.* **2019**, *13*, 116−122.
(15) Lum, D. J.; Mazurek, M. D.; Mikhaylov, A.; Parzuchowski, K. M.; Wilson, R. N.; Jimenez, R.; Gerrits, T.; Stevens, M. J.; Cicerone, M. T.; Camp, C. H. Witnessing the Survival of Time-Energy Entanglement Through Biological Tissue and Scattering Media. *Biomed. Opt. Express.* **2021**, *12*, 3658−3670.
(16) Shi, L.; Galvez, E. J.; Alfano, R. R. Photon Entanglement Through Brain Tissue. *Sci. Rep.* **2016**, *6*, 37714.
(17) Ono, T.; Okamoto, R.; Takeuchi, S. An Entanglement − Enhanced Microscope. *Nat. Commun.* **2013**, *4*, 2426.
(18) Israel, Y.; Rosen, S.; Silberberg, Y. Supersensitive Polarization Microscopy Using NOON States of Light. *Phys. Rev. Lett.* **2014**, *112*, 103604.
(19) Li, M.; Zou, C.-L.; Liu, D.; Guo, G. P.; Guo, G. C.; Ren, X. F. Enhanced Absorption Microscopy with Correlated Photon Pairs. *Phys. Rev. A* **2018**, *98*, No. 012121.
(20) Casacio, C. A.; Madsen, L. S.; Terrasson, A.; Waleed, M.; Barnscheidt, K.; Hage, B.; Taylor, M. A.; Bowen, W. P. Quantum-Enhanced Nonlinear Microscopy. *Nature.* **2021**, *594*, 201−206.
(21) Teich, M. C.; Saleh, B. E. A. Entangled−Photon Microscopy. *Ceskoslovensky Casopis Pro Fyziku.* **1997**, *47*, 3−8.
(22) Varnavski, O.; Goodson, T., III Two-Photon Fluorescence Microscopy at Extremely Low Excitation Intensity: the Power of Quantum Correlations. *J. Am. Chem. Soc.* **2020**, *142*, 12966−12975.
(23) Lee, D. I.; Goodson, T., III Entangled Photon Absorption in an Organic Porphyrin Dendrimer. *J. Phys. Chem. B* **2006**, *110*, 25582−25585.
(24) Upton, L.; Harpham, M.; Suzer, O.; Richter, M.; Mukamel, S.; Goodson, T., III Optically Excited Entangled States in Organic Molecules Illuminate the Dark. *J. Phys. Chem. Lett.* **2013**, *4*, 2046−2052.
(25) Varnavski, O.; Pinsky, B.; Goodson, T., III Entangled Photon Excited Fluorescence in Organic Materials: An Ultrafast Coincidence Detector. *J. Phys. Chem. Lett.* **2017**, *8*, 388−393.
(26) Dayan, B.; Pe'er, A.; Friesem, A. A.; Silberberg, Y. Two Photon Absorption and Coherent Control with Broadband Down-Converted Light. *Phys. Rev. Lett.* **2004**, *93*, No. 023005.
(27) Javanainen, J.; Gould, P. I. Linear Intensity Dependence of a Two-Photon Transition Rate. *Phys. Rev. A* **1990**, *41*, 5088−5091.
(28) Soule, H. D.; Vazquez, J.; Long, A.; Albert, S.; Brennan, M. Human Cell Line From a Pleural Effusion Derived From a Breast Carcinoma. *J. Natl. Cancer Inst.* **1973**, *51*, 1409−1416.
(29) Keydar, I.; Chen, L.; Karby, S.; Weiss, F. R.; Delarea, J.; Radu, M.; Chaitcik, S.; Brenner, H. J. Establishment and Characterization of Cell Line of Human Breast Carcinoma Origin. *Eur. J. Cancer.* **1979**, *15*, 659−670.
(30) de J Leon-Montiel, R.; Svozilık, J.; Salazar-Serrano, L. J.; Torres, J. P. Role of the Spectral Shape of Quantum Correlations in Two-Photon Virtual-State Spectroscopy. *New J. Phys.* **2013**, *15*, No. 053023.
(31) Burdick, R. K.; Varnavski, O.; Molina, A.; Upton, L.; Zimmerman, P.; Goodson, T., III Predicting and Controlling Entangled Two-Photon Absorption in Diatomic Molecules. *J. Phys. Chem. A* **2018**, *122*, 8198−8212.
(32) Kang, G.; Nasiri Avanaki, K. M.; Mosquera, M. A.; Burdick, R. K.; Villabona-Monsalve, J. P.; Goodson, T., III; Schatz, G. C. Efficient Modeling of Organic Chromophores for Entangled Two-Photon Absorption. *J. Am. Chem. Soc.* **2020**, *142*, 10446−10458.
(33) Fei, H. B.; Jost, B. M.; Popescu, S.; Saleh, B. E. A.; Teich, M. C. Entanglement-Induced Two-Photon Transparency. *Phys. Rev. Lett.* **1997**, *78*, 1679−1682.
(34) Parzuchowski, K. M.; Mikhaylov, A.; Mazurek, M. D.; Wilson, R. N.; Lum, D. J.; Gerrits, T.; Camp, C. H., Jr.; Stevens, M. J.; Jimenez, R. K. M. Setting Bounds on Entangled Two-photon Absorption Cross Sections in Common Fluorophores. *Phys. Rev. Appl.* **2021**, *15*, No. 044012.
(35) Grice, W. P.; Erdmann, R.; Walmsley, I. A.; et al. Spectral Distinguishability in Ultrafast Parametric Down-Conversion. *Phys. Rev. A* **1998**, *57*, R2289−R2292.
(36) Di Giuseppe, G. D.; Haiberger, L.; De Martini, F.; Sergienko, A. V. Quantum Interference and Indistinguishability with Femtosecond Pulses. *Phys. Rev. A* **1997**, *56*, R21−R24.
(37) Dayan, B. Theory of Two-Photon Interactions With Broadband Down-Converted Light and Entangled Photons. *Phys. Rev. A* **2007**, *76*, No. 043813.
(38) Zielnicki, K.; Garay-Palmett, K.; Cruz-Delgado, D.; Cruz-Ramirez, H.; O'Boyle, M. F.; Fang, B.; Lorenz, V. O.; U'Ren, A. B.; Kwiat, P. G. Joint Spectral Characterization of Photon-Pair Sources. *J. Mod. Opt.* **2018**, *65*, 1141−1160.
(39) Villabona-Monsalve, J. P.; Burdick, R. K.; Goodson, T., III Measurements of Entangled Two-Photon Absorption in Organic Molecules with CW-Pumped Type-I Spontaneous Parametric Down-Conversion. *J. Phys. Chem. C* **2020**, *124*, 24526−24532.
(40) Ekert, A.; Knight, P. I. Entangled Quantum Systems and the Schmidt Decomposition. *Am. J. of Phys.* **1995**, *63*, 415−423.
(41) Fedorov, M. V.; Miklin, N. I. Schmidt Modes and Entanglement. *Contemp. Phys.* **2014**, *55*, 94−109.
(42) Bennink, R. S.; Liu, Y.; Earl, D. D.; Grice, W. P. Spatial Distinguishability of Photons Produced by Spontaneous Parametric Down-Conversion with a Focused Pump. *Phys. Rev. A* **2006**, *74*, No. 023802.
(43) Bontemps, J.; Houssier, C.; Fredericq, E. Physico-Chemical Study of the Complexes of '33258 Hoechst' with DNA and Nucleohistone. *Nucleic Acids Res.* **1975**, *2*, 971−984.
(44) Bucevicius, J.; Lukinavicius, G.; Gerasimaite, R. The Use of Hoechst Dyes for DNA Staining and Beyond. *Chemosensors.* **2018**, *6*, 18.
(45) Shih, Y. Entangled Biphoton Source − Property and Preparation. *Rep. Prog. Phys.* **2003**, *66*, 1009−1044.
(46) Marjanovic, N. D.; Weinberg, R. A.; Chaffer, C. I. Cell Plasticity and Heterogeneity in Cancer. *Clin. Chem.* **2013**, *59*, 168−179.
(47) Villabona-Monsalve, J. P.; Varnavski, O.; Palfey, B. A.; Goodson, T., III Two Photon Excitation of Flavins and Flavoproteins with Classical and Quantum Light. *J. Am. Chem. Soc.* **2018**, *140*, 14562−14566.
(48) Dayan, B.; Pe'er, A.; Friesem, A. A.; Silberberg, Y. Nonlinear Interactions with an Ultrahigh Flux of Broadband Entangled Photons. *Phys. Rev. Lett.* **2005**, *94*, No. 043602.

https://doi.org/10.1021/acs.jpclett.2c00695
J. Phys. Chem. Lett. 2022, 13, 2772−2781

(49) Lukens, J. M.; Dezfooliyan, A.; Langrock, C.; Fejer, M. M.; Leaird, D. E.; Weiner, A. M. Demonstration of High-Order Dispersion Cancellation with an Ultrahigh-Efficiency Sum-Frequency Correlator. *Phys. Rev. Lett.* **2013**, *111*, 193603.
(50) Nechushtan, N.; Zhang, H.; Meller, M.; Pe'er, A. Optimal Detection of Ultra-Broadband Bi-Photons with Quantum Nonlinear SU(1,1) Interference. *New J. Phys.* **2021**, *23*, 113003.
(51) Pe'er, A.; Dayan, B.; Friesem, A.; Silberberg, Y. Temporal Shaping of Entangled Photons. *Phys. Rev. Lett.* **2005**, *94*, No. 073601.

https://doi.org/10.1021/acs.jpclett.2c00695
J. Phys. Chem. Lett. 2022, 13, 2772−2781